Stability of a Clamped Shallow Arch Subjected to Impulsive Loading

M. C. CHEUNG* AND C. D. BABCOCK JR.†
California Institute of Technology, Pasadena, Calif.

Clamped circular aluminum arches have been explosively loaded using a spray deposited light ignited explosive (Silver Acetylide-Silver Nitrate). Using high-speed photography and computerized data reduction, a detailed time history of the arch deflection has been obtained. This deflection was fitted with mode shapes in order to display the motion graphically. The experimental data shows that the clamped arch does not have a jump in response with increasing load level, but a transition from small displacement response to a large displacement response over a sizable range of load level.

Nomenclature

A = surface area of the arch, in.^{2}
E = Young's modulus, psi
h = arch thickness, in.
L = arch length, in.
I = specific impulse, lb-sec/in.^{2}
$\bar{I}$ = nondimensional impulse = $4I^2R^2/h^4E\rho$
P = static load
q_1,q_2,q_3 = generalized displacement coordinates
R = arch radius, in.
t = time, sec
w = arch displacement, in.
$W_{\max}{}^a$ = maximum nondimensional average displacement
W_e = weight of explosive, gm
α = independent variable, rad
β = arch half angle, rad
γ = geometric parameter = $L^2/4Rh$
ρ = mass density, lb sec^2/in.^{4}

I. Introduction

THE problem of dynamic buckling or nonlinear response of shell-like structures has been widely discussed in the past few years. The question of dynamic buckling is of concern since this phenomenon is associated with a large change in the structural response with a small change in the loading conditions. This change of response character with load is similar to the stability problem of static loading and hence the name dynamic buckling has often been adopted. However, since the loading and response are functions of time, the analogy is not quite complete. This has led to a variety of definitions of dynamic buckling.

As a result of the interest in this problem, much work has been done to determine simplified methods of finding the critical loading conditions without resorting to a direct solution of the time dependent nonlinear partial differential equations. This had led to methods of determining the relation between the static and dynamic buckling load for step loading.[1,2] Methods depending upon energy balances have also been developed.[3,4]

The shallow arch has been chosen as a model for many of these analytical studies. This rather simple structure has all of the nonlinear characteristics of much more complicated shell structures. A wide variety of this nonlinear behavior can be exhibited by changing the end conditions, loading or geometry of the arch.

From an experimental point of view, the clamped arch is the most practical problem when dynamic loading is used. Other boundary conditions are very difficult to duplicate in the laboratory. The clamped arch was the subject of a study by Humphreys.[5] His analysis used a Galerkin procedure and an analogue computer. In addition, he performed experiments using a clamped arch and sheet explosive.

The clamped arch was also considered by Simitses[4] who used an energy analysis. However, Vahidi[6] recently pointed out that the clamped arch under impulse loading does not have any equilibrium positions, stable or unstable, except the undeformed position. This situation can be explained more clearly if we examine the statically loaded arch for symmetric response (Fig. 1). The line OABC resembles a clamped arch and the line OA′B′C′ resembles a simply supported arch. At the zero lateral load condition, the simply supported arch has more than one equilibrium state. This means that if such an undeformed arch is impulsively loaded (given an initial velocity), the maximum response will have a sizable increase when the response just exceeds the equilibrium position D′. The character of the response will be completely different for a load level just below the critical impulse as compared to one just above. At the same time, a continuous increase of maximum response is anticipated for the clamped arch since other static equilibrium positions do not exist at zero load. The response character will not exhibit a drastic change at any impulse level and distinct dynamic buckling load cannot be

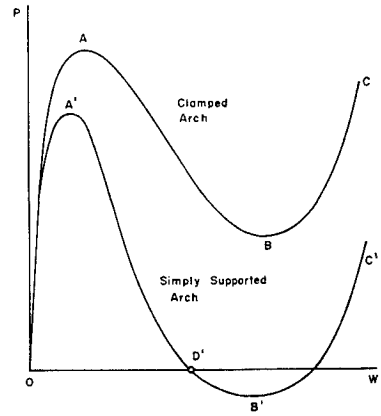

Fig. 1 Typical static response of arches.

Presented at the AIAA Structural Dynamics and Aeroelasticity Specialist Conference, New Orleans, April 14–17, 1969 (no paper number; published in bound volume of conference papers); submitted August 18, 1969; revision received January 28, 1970. The research in this paper was supported by the Air Force Office of Scientific Research, Office of Aerospace Research. United Air Force under Grant AFOSR 68-1424.

* Research Fellow of Aeronautics. Member AIAA.

† Associate Professor of Aeronautics. Associate Member AIAA.

distinguished. The nonexistence of equilibrium positions other than the undeformed one excludes the use of an energy analysis.

In order to clarify the behavior of the clamped arch under impulsive loading, the problem is re-examined in the report. Carefully controlled experiments have been carried out to obtain a time history of the arch motion after being explosively loaded. This data is then examined in detail and presented in a manner showing the difference in the behavior for this type of structure as opposed to the impulsively loaded simply supported arch.

II. Experiment

The experimental part of this work consisted of loading a clamped circular arch with a very short duration uniform pressure load. The resulting motion of the arch was recorded using high-speed photography. A detailed description of the experimental work is presented in the following sections.

1. Test Specimens

The equations that describe the motion of a shallow arch show that the circular arch can be characterized by one nondimensional parameter called γ in this report (see Fig. 2);

$$\gamma = L^2/4Rh = \beta^2 R/h$$

For all of the arches tested, the thickness was held constant and the same nominal radius of curvature was used.

The specimens were cut from $\frac{1}{16}$-in.-thick 2024 aluminum sheet, and were trimmed by the milling machine to $\frac{3}{4}$ in. wide. The strips were then rolled to approximately 30 in. radius in a three-roll roller. After rolling, the arches were heat treated. Tensile tests on curved specimens cut from the arches gave a Young's Modulus of 10.5×10^6 lb/in.^{2} and a proportional limit above 45,000 lb/in.^{2}

The arches are mounted into a heavy steel frame for testing. The ends are secured using Devcon B. An arch mounted in the frame is shown in Fig. 3.

2. Impulsive Load

Silver Acetylide-Silver Nitrate was used to apply a very short duration pressure loading on the arch. The advantage of this chemical is the low level of impulse possible, which is approximately one-tenth of commercially available sheet explosives. The general properties are introduced in Ref. 7. The explosive is produced in the form of a fine grained powder and is applied to the test specimen by spraying using acetone as a thinner.

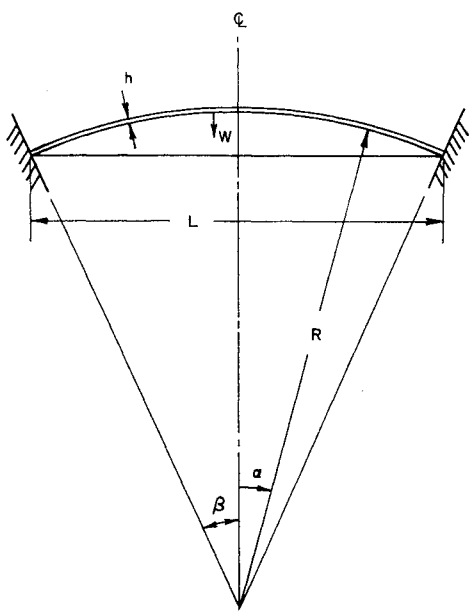

Fig. 2 Coordinate system of circular arch.

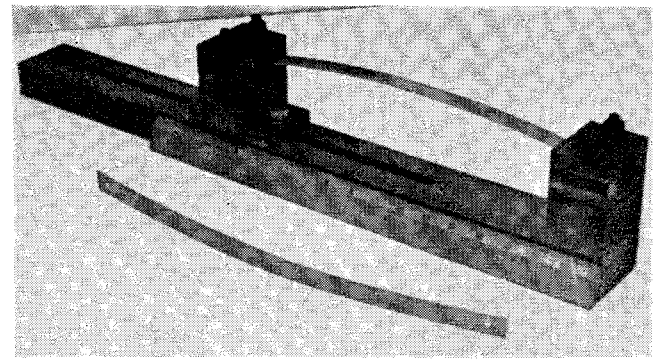

Fig. 3 Circular arch before and after installation in steel frame.

This explosive can be detonated by an electric spark or an intense light. It has been shown that a fairly large area can be detonated within a few -μsec if expendable Xenon flash tubes are used.[7] It was found that if one nonexpendable Xenon flash tube was used that complete detonation over the longest arch could be accomplished in less than 150 μsec. This duration of loading on the whole arch is short enough that it can be considered impulsive.

A GE-522 Xenon flash tube, mounted in a parabolic reflector, was used as the detonator. The tube was driven by a 250 microfarad capacitor charged to 5000 v. The rise time of the tube was about 20 μsec and the duration of the light pulse was of the order of 300 μsec.

The calibration of the impulse generated by this explosive was carried out on a ballistic pendulum. The explosive was deposited evenly on a 2-in.-square steel plate and attached to the end of the pivoted arm of the pendulum. The calibration curve of impulse vs weight is shown in Fig. 4. The offset

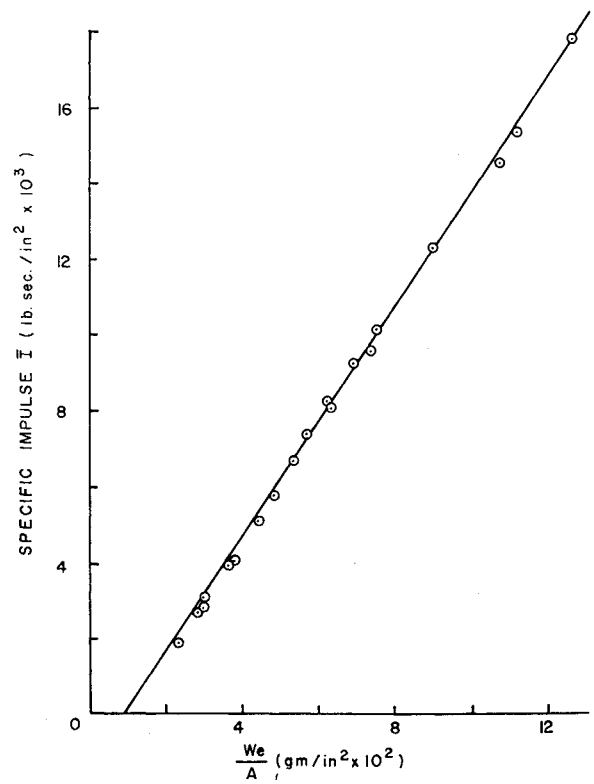

Fig. 4 Calibration of explosive (Silver Acetylide-Silver Nitrate).

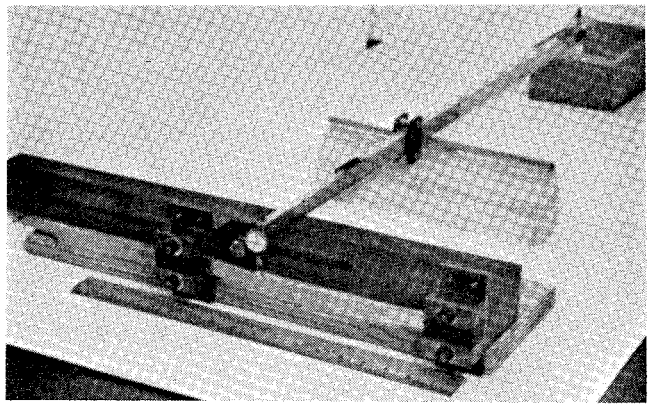

Fig. 5 Measuring of initial imperfection of circular arch.

from the origin is due to the friction at the pivot point. From this data an impulse level of 0.152 lb-sec/in.^{2}/g/in.^{2} (6.75×10^4 dyne-sec/cm^2/g/cm^2) was calculated. This is about 3.6% lower than previously found in Ref. 7.

3. Initial Imperfection Measurement

A pendulum like apparatus was built to measure imperfections of the arch. It consisted of a fixed center and rotatable arm which can be adjusted in length. A dial indicator with a a working range of 0.060 in. was installed at the tip of the arm (see Fig. 5).

The measurement was made by first adjusting the arm to the appropriate radius then pressing the concave side of the arch gently against the dial gauge. Starting from one end of the arch the dial gauge readings were taken at half-inch intervals along the arch until the dial gauge could not advance another full step. This gave the deviation of the arch shape from the preset radius. Applying the least-square method to the measured data the best fit radius and the best fit imperfection can be found.

Before the arches were mounted on the supports the imperfections were measured. Only those arches with imperfection amplitude less than five thousandths of an inch were used. Also, they were cut from longer ones so that the selected sections had a minimum amount of asymmetric imperfection. When the arch was mounted and the Devcon has hardened, the arch shape was measured again to make sure that it had not been excessively deformed due to the process of mounting.

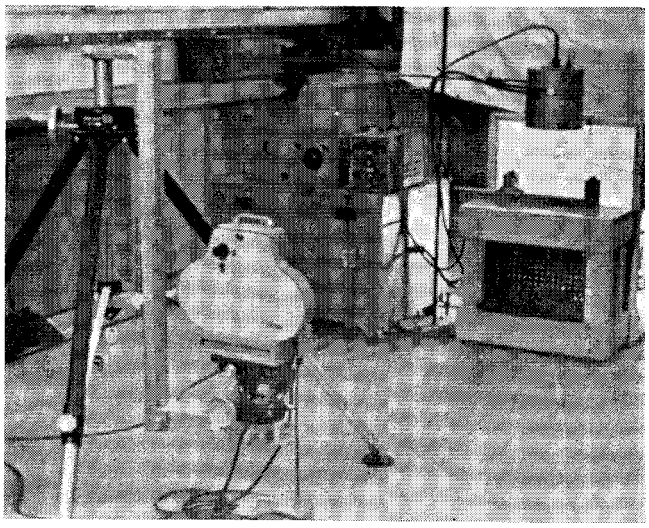

Fig. 6 Camera setup.

4. Camera Setup

A 16 mm, high-speed motion picture camera (HyCam, Red Lake Laboratories) was used to record the response of the arch. The axis of the camera was aligned perpendicular to the base line of the arch. To eliminate as much distortion as possible, the camera was placed at least 7 ft away.

The light was provided by four 1000 w quartz-iodine flood lamps. They were placed on the side of the arch opposite the camera and aimed directly at the camera. In order to collect more light at the camera, a large plastic Fresnel lens of focal length of 30 in. was placed between the arch and the lamps. A sheet of clear Mylar was placed on the flat side of the Fresnel lens to help diffuse the intense and unevenly concentrated light. A spot light meter at the camera position was used to check the evenness of the lighting of the Fresnel lens. The camera setup is shown in Fig. 6.

A 400 ft roll of Kodak Tri-X negative (ASA rating of 400) of standard thickness (0.006 in.) was used for each test shot. However, the desired framing rate of 10,000 pictures per sec was only obtained on the last 100 ft of film. The exact framing rate was determined by a timing light which exposed a small dot of light on the edge of the film every $\frac{1}{1000}$ of a second.

5. Response Measurement

A detailed deflection history of the arch motion was obtained by reading the film frame by frame. The film was projected using a 500 w slide projector on a mirror at a distance of about 15 ft. The image was reflected to a screen ruled with 21 equally spaced lines (Fig. 7). The distance to the mirror was adjusted until the arch image from support to support fix exactly on the twenty equal division on the screen. The lines then serve as the X coordinate for the arch. The Y distance was measured using a stretched wire perpendicular to the X lines. This wire was attached to a moving slide whose position was measured by a linear potentiometer. The wire was carefully moved to each intersection of the arch image and the lines ruled on the screen. The potentiometer reading was automatically recorded on punched cards for digital computer reduction. Approximately 50 frames were read for each test covering about 10 msec of motion.

6. Test Procedure

When a particular value of γ had been selected, the arch was cut to the appropriate length. The surface of the arch was then cleaned and the weight determined to the nearest $\frac{1}{2000}$ of a gram. An estimation of the weight of the explosive was made and then it was sprayed on the convex side of the arch. The explosive was cured for one hour at 100°F. The arch and the explosive are then weighed and the amount of deposited explosive determined. If the correct amount is not obtained the process was repeated until the weight differs from

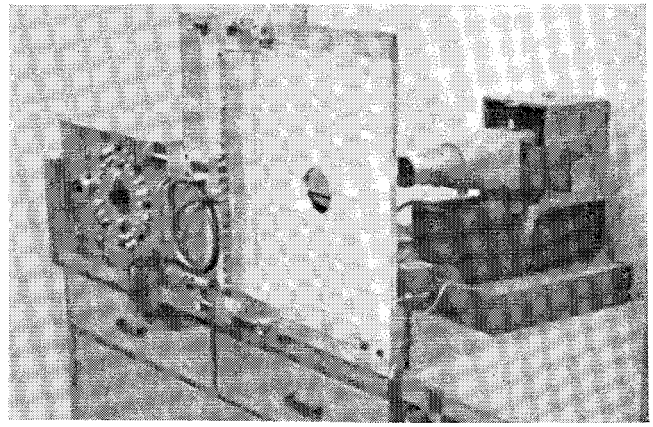

Fig. 7 Film reader to measure deformed arch shape.

Table 1 Geometric description of tested arches

Arch	Thickness, in.	Radius, in.	Length, in.	γ
B9	0.0623	31.76	8.64	9.43
B6	0.0623	30.22	8.43	9.44
B7	0.0622	25.45	8.13	10.44
B8	0.0623	32.33	8.57	9.12
C3	0.0605	31.31	12.08	19.25
C2	0.0605	31.57	12.20	19.48
C5	0.0605	30.55	12.28	20.40
C4	0.0605	28.10	12.12	21.60
C8	0.0604	29.47	12.03	20.33
C7	0.0604	26.64	12.11	22.79
C9	0.0603	31.84	12.31	19.73

that desired by a few hundredths of a gram. Next the arch was secured in the steel frame with Devcon B.

After the Devcon has hardened, the arch and support are aligned with the camera. The camera was started and an Event Synchronizer built into the camera discharges the Xenon tube when 325 ft of film has been exposed. The deformation of the arch that is of interest takes about 3 ft of film. The last 100 ft of exposed film was developed and the part of interest retained.

III. Test Results

A total of 11 tests were recorded by the high-speed camera. These tests were divided into two groups. Group B had a geometric parameter close to 10 and for group C, γ was close to 20. The dimensions are listed in Table 1. The arches used for testing were selected so as to minimize the size of initial imperfections. In all cases the deviation from the perfect arch was less than 5% of the thickness.

A typical high-speed photographic record is printed in Fig. 8. The sequence starts from the top of the left hand column. The time between frames is one tenth of a millisecond. After the deformed shapes were measured, the response of the arch was examined in several manners. First, a three modes approximation to the deformed shape was calculated. The representation used is as follows:

$$w = (1 - \alpha^2/\beta^2)^2[q_1(t) + (\alpha/\beta)q_2(t) + (\alpha^2/\beta^2)q_3(t)]h$$

The coefficients were determined by using a least-square fit of the experimental data from the high-speed pictures. The time history of the three modes is shown in Fig. 9 for a typical test. The trajectories in a q_1, q_3 space can also be displayed. Figure 10 shows a supercritical and subcritical response for each group of arches. The line of average displacement (defined later) equal to one is also shown in the figures.

Finally, the average displacement was calculated for the time of response of interest. This displacement is defined as the area between the deformed and undeformed arch. It is normalized to the area enclosed by the undeformed arch and the base line. The values of the maximum average displacement are listed in Table 2 and are shown in Fig. 11 as a function of the nondimensional impulse $\bar{I}$. This figure shows that the arch exhibits a large increase in rate of change of response over a rather small range of impulse level. Although the interpretation of the data is not precise, it appears that a distinct jump of maximum response does not occur. As pointed out in the introduction, this jump should not be expected for clamped arch under impulse loading. The maximum rate of change of response (the inflection points for the faired curves in Fig. 11) is at an impulse level $\bar{I}$ of 9 and 22 for γ equal to 10 and 20, respectively. It is interesting to note that these points are close to the point of average displacement equal to one, which was used by Humphreys[5] to define the critical load. However, they are about 6–7 times as high as Humphreys' experimental results. The reason for this is not known at this time.

Table 2 Summary of impulse tests

Arch	W_e/A, g/in.^{2}	$\bar{I}$	W_{max}[a]
B9	0.0626	8.43	0.5596
B6	0.0749	10.45	1.3905
B7	0.0964	12.19	1.5830
B8	0.0847	14.82	1.7342
C3	0.0742	12.60	0.2281
C2	0.0799	15.08	0.3616
C5	0.0826	16.66	0.3969
C4	0.0854	16.95	0.4669
C8	0.0962	20.33	0.6239
C7	0.1098	21.65	0.9185
C9	0.1037	27.75	1.6277

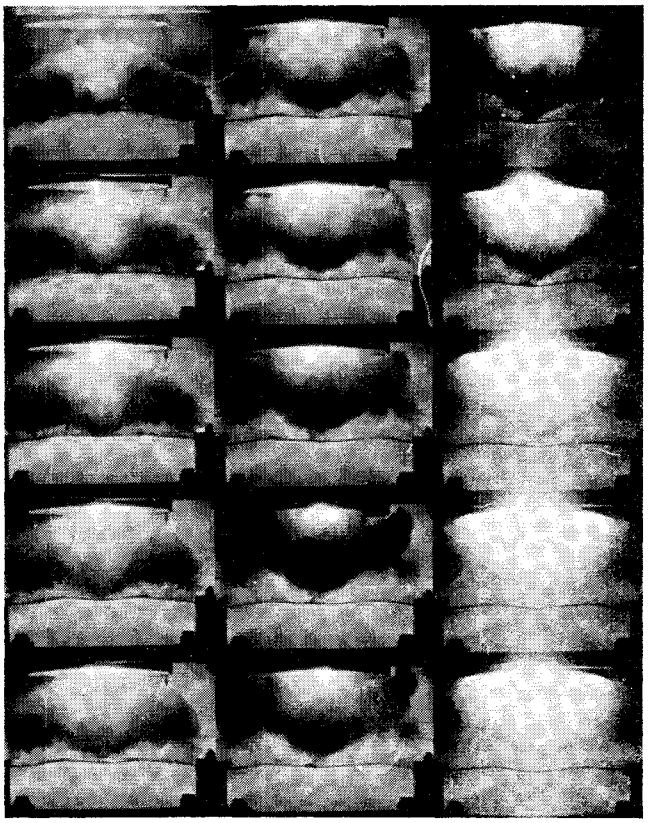

Fig. 8 A typical high-speed photographic record.

In addition to the dynamic test results described previously, an attempt was made to determine the static equilibrium positions of the clamped arch. This is of interest since the exis-

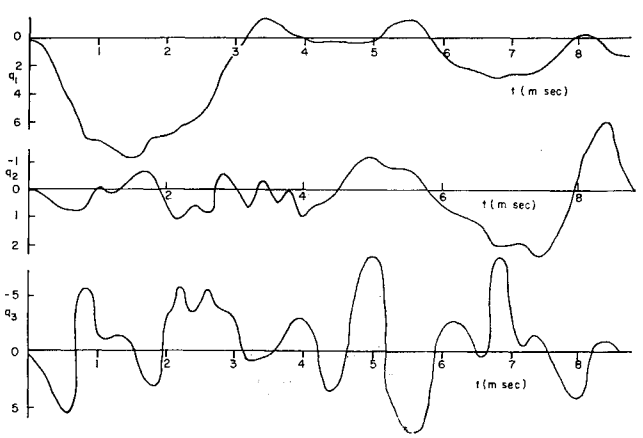

Fig. 9 Response of arch B8, $\bar{I}$ = 14.82.

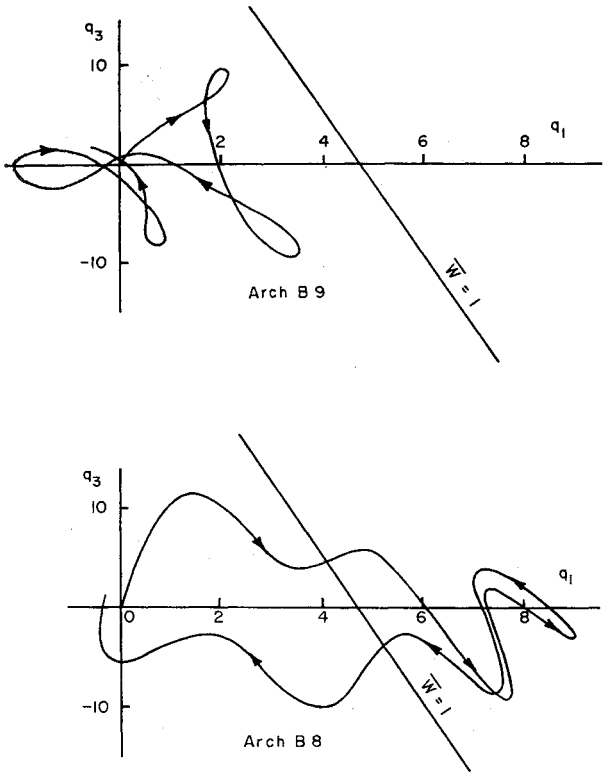

Fig. 10a Trajectories of arches for $\gamma \approx 10$.

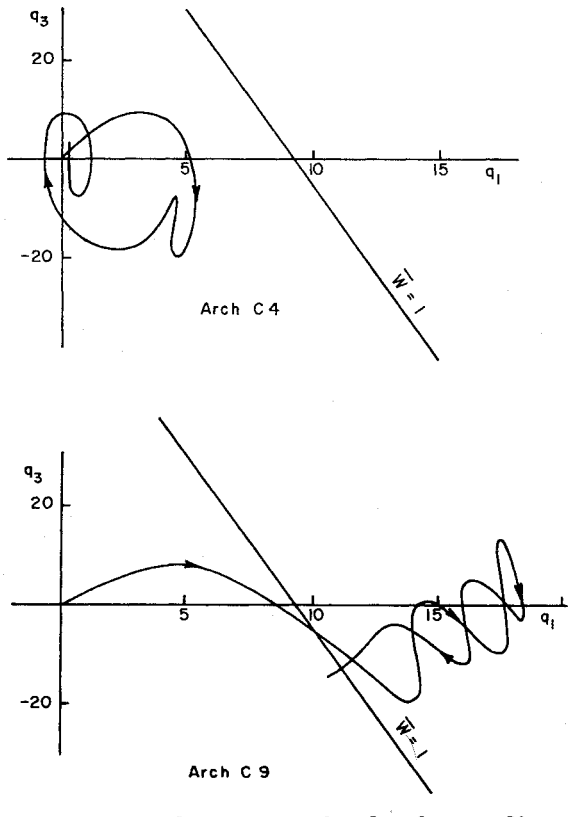

Fig. 10b Trajectories of arches for $\gamma \approx 20$.

tence of these positions is a requirement in an energy approach for determining the dynamic buckling loads. These tests were carried out by pushing the arch through to a large displacement configuration by hand and attempting to find a position where it would stay. This was unsuccessful for the four arches used with $\gamma \approx 10$ and 20. In addition, the existence of an unstable equilibrium position could not be detected.

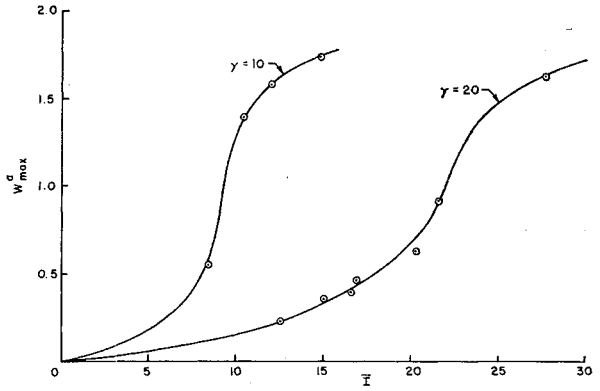

Fig. 11 Impulse vs maximum average displacement for clamped arch.

This is somewhat more difficult to determine experimentally since it is like trying to balance a ball on top of a hill. However, there did not seem to be any equilibrium points other than the undeformed position for the arch tested. This is in agreement with Vahidi's calculation.[6]

IV. Conclusion

The experimental work on the impulsively loaded clamped arch shows that the maximum response has a significant increase in value for a small increase in load at some value of impulse. It would appear for the data available that this increase is a smooth transition from a small response to a large response at some critical impulse level. Therefore, the use of a definition of dynamic buckling which requires a finite change in response for an infinitesimal increase in load would not consider this problem as a dynamic buckling problem. However, from a practical point of view the increase in deflection is of the order of three for a small increase in impulse level. This increase is about the same amount as one obtains for step loading on a simply supported arch in the range of geometric parameter where direct snapping occurs.[8]

It is of interest to note that this problem is like the one of direct snapping as categorized by Lock.[9] In other words the structure reaches its maximum displacement on the first oscillation of the fundamental mode. This can be seen from the response plot (Fig. 9) combined with the trajectories (Fig. 10). An examination of the nonsymmetric response shows that it does not appear to be parametrically excited by the symmetric mode as is characteristic of indirect snapping.

In summary, while no evidence has been found that the clamped circular arch under impulse loading can be rigorously categorized as a dynamic buckling problem, it is clear that over a small range in impulse the arch undergoes a significant increase in response. It is therefore of practical significance to determine this range of impulse. In addition, it was experimentally determined that no stable equilibrium position exists for the clamped arch free from lateral load other than the undeformed position. Also, the existence of an unstable equilibrium position was not detected.

References

[1] Budiansky, B., "Dynamic Buckling of Elastic Structures: Criteria and Estimates," *Dynamic Stability of Structures*, edited by G. Herrmann, Pergamon Press, 1967, pp. 83–106.

[2] Hutchinson, J. W. and Budiansky, B., "Dynamic Buckling Estimates," *AIAA Journal*, Vol. 4, No. 3, March 1966, pp. 525–530.

[3] Hsu, C. S., "On Dynamic Stability of Elastic Bodies with Prescribed Initial Conditions," *International Journal of Engineering Science*, Vol. 4, March 1966, pp. 1–21.

[4] Simitses, G. J., "Dynamic Snap-Through Buckling of Low

Arches and Shallow Spherical Caps," Ph.D. dissertation, June 1965, Stanford Univ., Calif.

[5] Humphreys, J. S., "On Dynamic Snap-Buckling of Shallow Arches," *AIAA Journal*, Vol. 4, No. 5, May 1966, pp. 878–886.

[6] Vahidi, B., "Non-Existence of Snap-Through for Clamped Shallow Elastic Arches Subjected to Impulsive Load," TR 8, March 1969, Univ. of California, San Diego.

[7] Hoese, F. O., Langner, C. G., and Baker, W. E., "Simultaneous Initiation over Large Areas of a Spray Deposited Explosive," *Experimental Mechanics*, Sept. 1968, pp. 392–397.

[8] Lock, M. H., "The Snapping of a Shallow Sinusoidal Arch under a Step Pressure Load," *AIAA Journal*, Vol. 4, No. 7, July 1966, pp. 1249–1256.

[9] Lock, M. H., "A Study of Buckling and Snapping under Dynamic Loads," TR-0158(3240-30)-3, Dec. 1967, Aerospace Corp.

AUGUST 1970 AIAA JOURNAL VOL. 8, NO. 8

Initial Temperature and Pressure Effects on Composite Solid-Propellant Burning Rates: Comparisons with Theory

DAVID W. BLAIR*
Polytechnic Institute of Brooklyn, Brooklyn, N. Y.

Pressure vs burning rate data are presented for an ammonium perchlorate composite solid propellant at four levels of initial temperature. For each level of initial temperature the data are fitted by least squares to the equation $P/r = a + bP^N$. Three values of N are considered at each temperature level, $N = 1$, $N = \frac{2}{3}$ and $N =$ value for best fit to the data. These fits are then used to evaluate the relative merits of two burning rate laws, $N = 1.00$ corresponding to a law that includes the axisymmetric jet diffusion flame theory and $N = \frac{2}{3}$ corresponding to the Summerfield granular diffusion flame theory. The relative variation of the parameters a and b with temperature is compared with the expectation of the Summerfield theory. It is concluded that although $N = \frac{2}{3}$ gives a superior fit to $N = 1.00$, no law of the type $P/r = a + bP^N$ fits the data without systematic error and that the variation of best fit N with initial temperature casts doubt upon the physical model underlying both burning rate laws. The burning rate law suggested by Fenn, $P/r = a + brP^N$ also is tested. Its best fit is superior to that for $N = 1$ in the previous equation but it is inferior to the fit of that law for $N = \frac{2}{3}$ or N taken as the best fit value.

Nomenclature

- a = gas phase reaction time parameter or first adjustable parameter
- A = Arrhenius prefactor
- b = diffusion time parameter or second adjustable parameter
- C_s = specific heat of solid propellant
- D = gas phase binary diffusion coefficient
- E = activation energy
- M_g = average molecular weight of the gas phase
- N = pressure index in equation for P/r
- P = absolute pressure, psia in data
- Q_s = heat released in the solid phase
- R = gas constant per mole
- r = burning rate, in./sec in data
- T_g = effective absolute temperature of the combusting gases
- T_o = initial absolute temperature of the solid propellant (this is given as °F in the data but it appears always in the theories as degrees absolute)
- T_s = absolute temperature of the burning surface of the solid propellant
- T_1 = absolute temperature of the flame
- ρ_s = density of the solid propellant
- λ_g = thermal conductivity of the gas phase at the solid surface
- μ = average oxidizer particle size

Received May 5, 1969, revision received November 13, 1969. This work is based upon a re-examination of previously unpublished data from experiments that the author performed in the laboratories of M. Summerfield at Princeton University during the period 1960–1961. He gratefully acknowledges the support that he received during that period. Thanks are also due W. R. Allen of the Polytechnic Institute of Brooklyn for his helpful suggestions regarding the treatment of the data and to G. K. Berge of the same institution for making time available for the necessary calculations on the data-net system.

* Associate Professor of Mechanical Engineering; presently Senior Research Engineer, Corporate Research Laboratories, Esso Research and Engineering Company, Linden, N.J.

Introduction

PERHAPS the most successful theory of the steady-state burning rates of ammonium perchlorate composite solid-propellants is the granular diffusion flame theory of Summerfield.[1] It is a rather intuitive theory based upon a plausible model of the propellant gas phase flame structure, the details of which are extremely resistant to precise experimental investigation. Because the assumed flame structure has not been definitively investigated experimentally, the principal verification of the theory rests upon its agreement with such readily determined propellant characteristics as the variation of burning rates with pressure and with oxidizer particle size and particle size distribution. With regard to the effects of pressure the theory is quite explicit. This dependence is given as

$$1/r = (a/P) + b/P^{1/3} \tag{1}$$

The constants a, the "gas-phase reaction time parameter," and b, the "diffusion time parameter," although independent of pressure are functions of other physical variables, including temperature, as will be discussed later. Equation (1) is formed by assuming that the gas phase flame zone thickness